Systematic Analysis Methodology for Mobile Phone's Electrostatic Discharge Soft Failures

Ki Hyuk Kim, *Member, IEEE*, and Yongsup Kim

***Abstract*—A systematic analysis methodology for mobile phone's electrostatic discharge (ESD) soft failures is proposed. The proposed analysis methodology consists of two parallel processes: one is the ESD simulation and the other is the ESD characterization of the mobile phone. The ESD simulation models that consist of the ESD generator, the ESD testing setup, and a mobile phone are also developed and their accuracy is experimentally verified. The proposed methodology is applied to design the countermeasures against the ESD soft failure of the slide-type mobile phones and the root causes of the ESD soft failures are analyzed. The *RC* low-pass filters are designed to improve the ESD immunity of the mobile phone and the ESD simulation results of the improved mobile phone show more than 82% voltage-level reductions of the signals, which cause the ESD soft failures. In order to verify that the reduced voltage levels, actually, solve the problem of ESD soft failures, the improved mobile phone's ESD immunity is characterized again, and no ESD soft failure is detected.**

***Index Terms*—Digital circuits, electromagnetic analysis, electromagnetic interference, electrostatic discharge (ESD).**

I. Introduction

SINGLE chip/package solutions using the system-on-chip or the system-on-package technology in which the RF, power, analog, and digital blocks are all embedded in a single chip/package are now commercially available [1]. Extensive research is currently being carried out to apply such single chip/package solutions to multifunctional portable devices such as mobile phones, smart phones, and multimedia players.

However, from the point of designing devices without electrostatic discharge (ESD) failures, there are a few side effects of adopting the single chip/package solutions. A high level of ESD causes damage to interconnections and CMOS devices because the breakdown voltages of the scaled CMOS devices are lowered [2]. The scaled devices are more vulnerable to external ESD due to these devices' high cutoff frequencies [3]. In addition, there is a higher probability that the operations of the CMOS devices are, simultaneously, affected by ESD because multiple devices are packed into a single chip/package.

The system-level failures caused by ESD are divided into two categories [4]: 1) ESD hard failures; and 2) ESD soft failures.

Manuscript received November 2, 2010; revised March 11, 2011; accepted April 9, 2011. Date of publication May 16, 2011; date of current version August 18, 2011.

The authors are with the Advanced CAE Laboratory, Digital Media and Communications R&D Center, Samsung Electronics Company, Ltd., Suwon 443-742, Korea (e-mail: kihyuk93.kim@samsung.com; yongsup2.kim@samsung.com).

Color versions of one or more of the figures in this paper are available online at http://ieeexplore.ieee.org.

Digital Object Identifier 10.1109/TEMC.2011.2143719

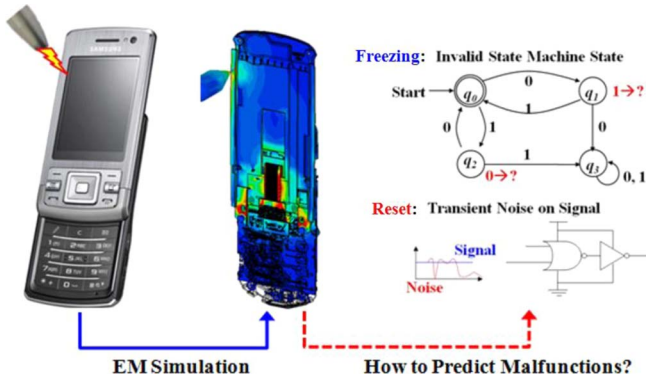

Fig. 1. Bottlenecks of ESD soft failures analysis using EM-software-based analysis techniques.

The root causes of the ESD hard failures are easier to analyze than those of the ESD soft failures because it is possible to trace back their causes by finding the locations of the electromigrations of the interconnections or the device breakdowns using the IC decapsulation technique. However, it is difficult to find the root causes of the ESD soft failures because they are temporary events and the system can recover to its normal state after rebooting the system. Freezing (lockup), reset, power-off, and an abnormal display status of the system are typical examples of the ESD soft failures.

In a previous study [5], the localized near-field scanning method was applied to systematically analyze the system-level ESD soft failures. However, due to the large size of the field injection probes, it is difficult to pinpoint the root causes, especially, when high-density IC packages such as the ball grid array or chip scale package are used and signal traces are routed on the inner layer of printed circuit boards (PCBs). In addition, the relationship between the injected near-field strengths and the induced-field strength of the IC when performing the system-level ESD testing based on the IEC 61000-4-2 standard [6] is not defined.

Analysis techniques using electromagnetic (EM) software are widely applied to design mobile phones, and are currently the best approach to analyze the ESD current paths on mobile phones. However, the ESD soft failures of mobile phones cannot be completely analyzed using these techniques. The ESD current paths are governed by EM field theory and are predicted using the EM software, as shown in Fig. 1. However, the ESD soft failures occur only when the ESD, which influences the signals of the ICs, causes malfunctions of the internal circuits. For example, if the mobile phone is in the $q1/q2$ state and the ESD makes the input level of the $q1/q2$ state 1/0, then the mobile

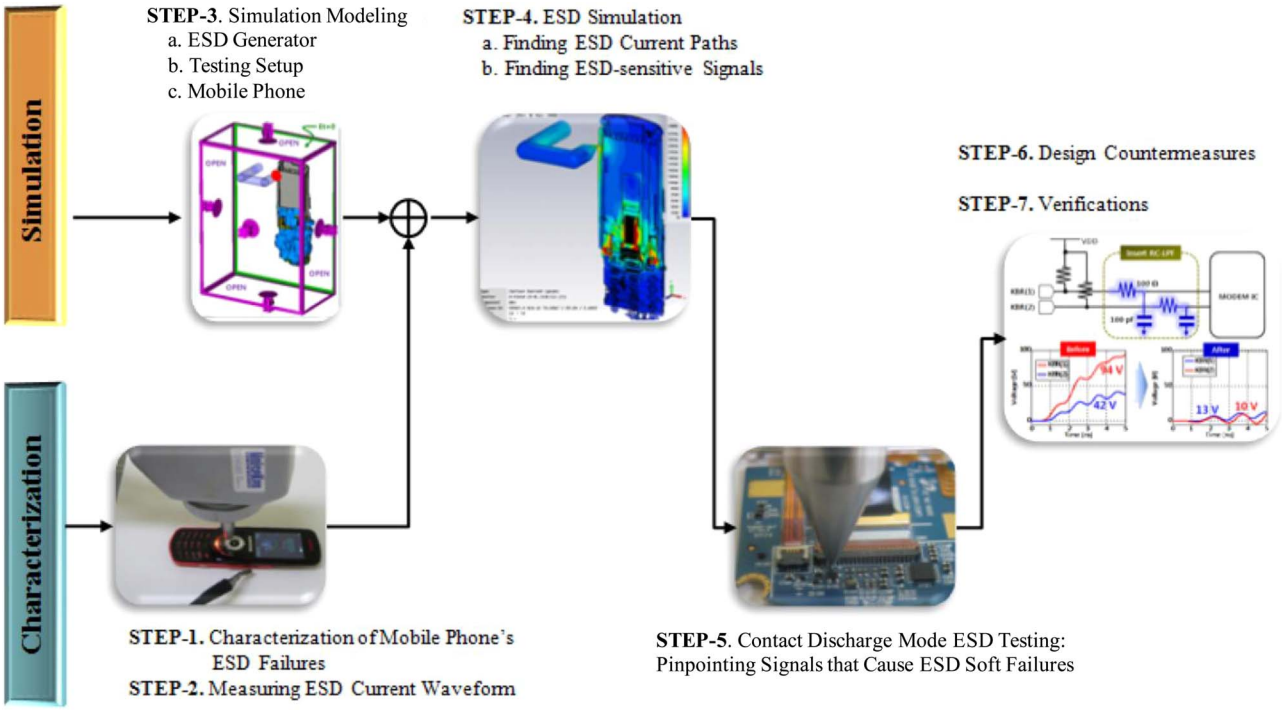

Fig. 2. Workflow of the proposed analysis methodology for mobile phone's ESD soft failures.

phone will be frozen because there is no predefined transition for the $q1/q2$ state with the input level of 1/0 as shown in Fig. 1. If the reset signal that is typically an active low signal is contaminated by the ESD and goes down to the logic level 0, then the system will be rebooted. These kinds of malfunctions cannot be predicted using the EM software.

In this paper, a systematic analysis methodology for the mobile phone's ESD soft failures is proposed. In Section II, the analysis methodology that consists of the ESD simulation and the ESD characterization processes is proposed. The modeling methods of the mobile phone, the ESD generator, and the ESD testing setup for the ESD simulations are explained in Section III. In order to validate the modeling accuracy, experimental verifications are conducted, and the results are discussed. The proposed analysis methodology is applied to improve a slide-type mobile phone's immunity to ESD soft failures. The case study is addressed in Section IV followed by the conclusion in Section V.

II. Systematic Analysis Methodology for Improvement of Mobile Phone's ESD Immunity

The workflow for the proposed systematic analysis methodology is shown in Fig. 2. The analysis methodology consists of two parallel processes, i.e., one is the ESD simulation and the other is the ESD characterization of the mobile phone, as shown in the top and bottom of Fig. 2, respectively.

First, the characterization of the mobile phone's ESD soft failures is carried out (STEP-1) based on the international ESD testing standard IEC 61000-4-2 [6]. The ESD soft failures of the mobile phone are detected in this step.

For accurate ESD simulations, it is important to excite the ESD simulation model using the measured ESD current waveform because the ESD current paths are dependent on the frequency components of the ESD current. The ESD current waveform of the ESD generator is measured using a commercial current probe (STEP-2).

The modeling steps for the ESD generator, the ESD testing setup, and the mobile phone are followed (STEP-3), and the details of the modeling methods are explained in Section III.

The goals of the ESD simulations are to find the ESD current paths on the mobile phone and ESD-sensitive signals for which the voltage and current levels are greatly changed by the ESD. A commercial time-domain EM field solver is used for the ESD simulations (STEP-4).

However, the ESD-sensitive signals may or may not cause ESD soft failures. ESD soft failures occur only when the ESD current that influences the ESD-sensitive signals causes a malfunction of the ICs, which cannot be predicted using the EM software. In order to pinpoint which of the ESD-sensitive signals cause the ESD soft failures, contact discharge mode ESD testing is performed on the ESD-sensitive signals (STEP-5). The contact mode discharge on the signals of the ICs is not in agreement with the IEC 61000-4-2 standard; however, by exciting the ESD-sensitive signals with the ESD current from the ESD generator, the signal (signals) that causes (cause) the ESD soft failures is (are) pinpointed among the ESD-sensitive signals. The internal resistance (330 Ω) and the capacitance (150 pF) of the ESD generator do not disturb the normal operations of the signals, because the ground return cable of the resistor and capacitor is connected to the ground reference plane (GRP) while the mobile phone is on the horizontal coupling plane (HCP).

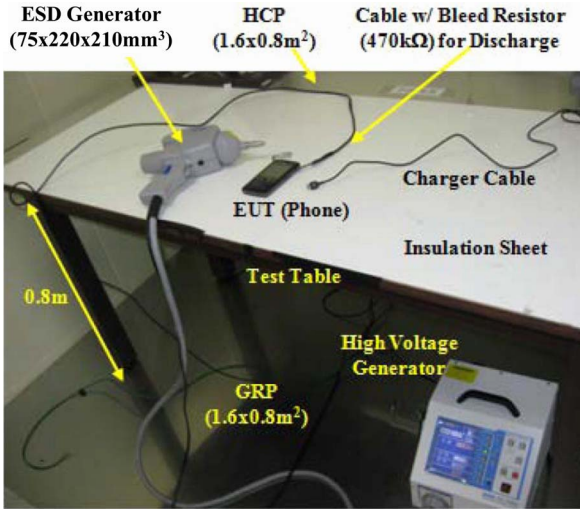

Fig. 3. ESD testing setup for the ungrounded EUT.

The GRP and HCP are electrically isolated with two 470 kΩ bleed resistors.

Countermeasures against ESD soft failures are devised for the pinpointed signals (STEP-6) and are subsequently verified (STEP-7).

III. ESD Simulation Modeling for ESD Generator, ESD Test Setup, and Mobile Phones

A. ESD Testing Setup for Ungrounded Equipment Under Test

Fig. 3 shows the ESD testing setup for the ungrounded equipment under test (EUT) based on the international ESD testing standard IEC 61000-4-2 [6], which is used for the ESD testing of battery-operated devices such as mobile phones. The EUT is on the HCP and the insulation sheet with the dielectric constant of 3.4 and the thickness of 0.5 mm is placed between the HCP and the EUT.

The ESD testing of the mobile phone consists of three steps. The first step involves discharging of the mobile phone using the ESD generator. Next, the responses of the mobile phone are examined to detect the occurrence of ESD soft failures. The final step is bleeding off the ESD current on the mobile phone because the ESD charges on the mobile phone should be discharged before the next ESD testing. These three steps are repeated until the entire surface of the mobile phone is tested. Based on our company's internal regulations, only the air discharge mode ESD testing is performed.

B. Simplified ESD Simulation Models for ESD Generator

Typical widths of the digital signal traces on the PCBs of the mobile phones are 0.1 mm, while the dimensions of the ESD generator are 75 (W) × 220 (H) × 210 (D) mm^3 [7]. In addition, for the full 3-D modeling of the ESD generator, the operation of the relay and the nonlinear behavior of the ferrites in the ESD generator should be considered in the simulation model [8]. It is inefficient to use the full 3-D ESD generator model for the system-level ESD simulations because a large size of the meshes and modeling of nonlinear materials are required.

TABLE I
Comparisons of ESD Generator Simulation Models [8]

	Full 3-dimensional Model	Simplified Model
Injected ESD Current	Accurate	Accurate
H-field	Accurate	Accurate Closed to EUT
E-field	Accurate	Not Correct
Strap Current	Accurate	NA
Radiation Caused by ESD Generator	Included	Not Included
Calculation Time	Long	Short

On the other hand, the simplified ESD generator model with the measured ESD current source requires a much smaller size of the meshes; however, it can reproduce only the ESD current and the H field near the tip caused by the injected ESD current. The effects of the E and H fields from the ESD generator and the ground strap current are not included in the simplified ESD generator model. The pros and cons of the ESD generator models are tabulated in Table I [8].

In essence, we would like to use the simplified ESD generator model; however, the simplified model is applicable only when the influence of the inject current and the H field near the tip is dominant, and the influences of the other components such as the E and H fields from the ESD generator and the ground strap current can be ignored. In order to find which component (components) is (are) the dominant cause (causes) of the ESD soft failures, the mobile phones are tested with two different ESD testing conditions and the responses of the mobile phones are compared. Fig. 4(a) shows the conventional ESD testing condition under which the ESD injected current as well as the E and the H fields from the ESD generator and the ground strap current affect the mobile phone's operations, while Fig. 4(b) shows the ESD testing condition under which the ESD current bypasses the mobile phone and only the E and H fields from the ESD generator and the ground strap current can cause the ESD soft failures. The ESD generator ESS-2000AX from Noiseken, Inc., Kanagawa, Japan, [7] with the charging voltage of +8 kV is used and the air discharge mode ESD testing is performed 100 times. The influence of the H field near the tip is not considered in the experiments, because the simplified ESD generator model can reproduce the H field near the tip as well as the injected ESD current.

It is important to note that the lightning rod with the dummy load is placed near the mobile phone in Fig. 4(b) in order, for the ESD generator, to generate the same ESD current. The measured ESD current waveforms of each testing condition are also shown in Fig. 4(a) and (b) and are in close agreement with each other.

Three types of mobile phones are tested, and the ESD testing results are tabulated in the "Mobile Phone #1," the "Mobile Phone #2," and the "Mobile Phone #3" rows, respectively, in Table II. The experiments indicate that the mobile phone's ESD

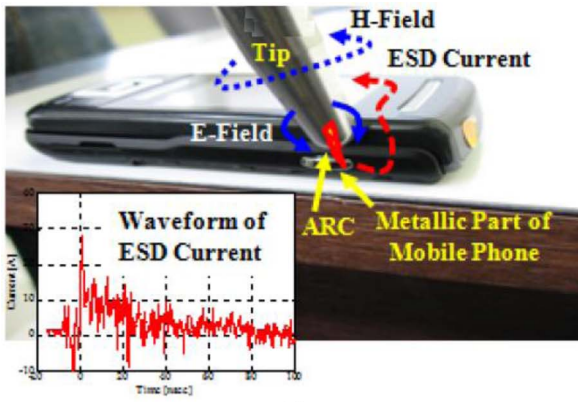

(a)

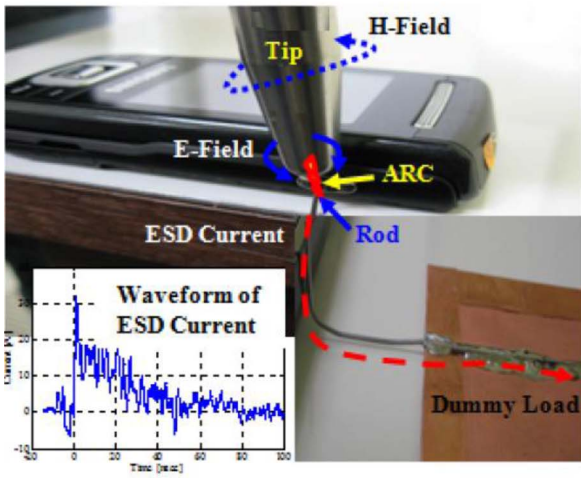

(b)

Fig. 4. ESD testing conditions to find causes of mobile phone's ESD soft failures. (a) Conventional ESD testing condition. (b) ESD current bypasses the mobile phone.

TABLE II
ESD TESTING RESULTS WITH TESTING CONDITIONS AS SHOWN IN FIG. 4

	Conventional (shown in Fig. 4-(a))	ESD Current Bypasses Mobile Phone (shown in Fig. 4-(b))
Candidates for ESD Soft Failures	Injected ESD Current, E and H Fields from Generator and Ground Strap Current	E and H Fields from Generator and Ground Strap Current
Mobile Phone #1	PWR-OFF	No ESD Failure
Mobile Phone #2	Freezing Followed by RESET	No ESD Failure
Mobile Phone #3	PWR-OFF	No ESD Failure

soft failures are caused by the injected ESD current and that the effects of the other components are negligible. Based on the experimental results, the simplified ESD generator model with the measured ESD current waveform is used for the following system-level ESD simulations.

Because the ESD current paths are determined by the frequency components of the ESD current, the measured ESD current waveform is used instead of the standard IEC 61000-4-2 current waveform [6]. The digital sampling oscilloscope

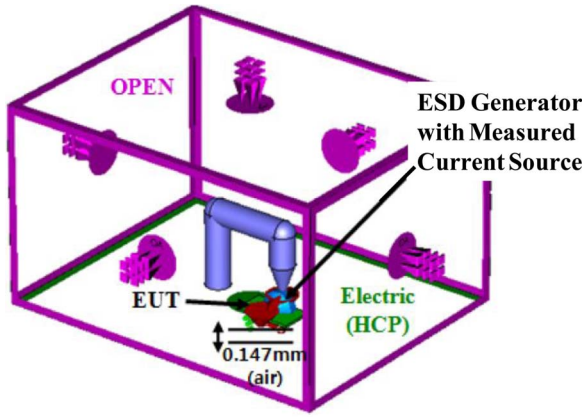

(a)

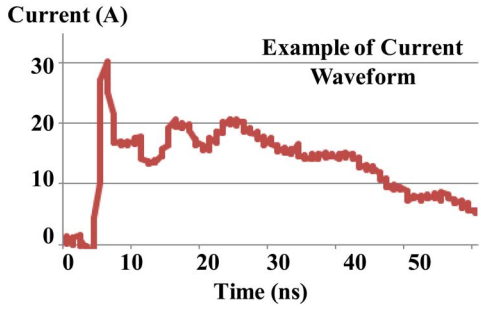

(b)

Fig. 5. (a) ESD simulation models of the ESD generator and the ESD testing setup. (b) Example of measured current waveform.

TDS3054B from Tektronix, Inc., Beaverton, OR [9], which has a 500-MHz bandwidth and a 5.0 Gsample/s sampling rate, is used to measure the ESD current waveform, and the high power attenuator BW-40N100 W from minicircuits [10], which has a 40-dB attenuation factor and a 100-W rated power, is used to protect the oscilloscope. The current probe F-65 from Fischer Custom Communications, Inc., Torrance, CA [11], which has a transfer impedance of 1 Ω from 1 to 1000 MHz, is used to measure the ESD current waveform.

C. Simplified ESD Simulation Models for the Testing Setup

The ESD simulation models of the testing setup are simplified based on the principle that the mobile phone and the HCP form a 3-D capacitor and the transient current paths are determined by their 3-D structures. The GRP, the connection cable, and the bleed resistors are not included in the ESD simulation model because the HCP is the reference plane in the case of the small EUTs such as mobile phones. The perfect-E boundary condition is used to model the HCP. The insulation sheet that is between the EUT and the HCP and has the dielectric constant of 3.4 and the thickness of 0.5 mm is equivalently modeled as the air gap with the thickness of 0.147 mm without using a 3-D object.

Fig. 5(a) shows the developed ESD simulation models of the ESD generator and the ESD testing setup. An example of the measured ESD current waveform is shown in Fig. 5(b).

D. Simplified ESD Simulation Models for Mobile Phones

Mobile phones consist of active components such as baseband modems, power management ICs, multimedia processors, ESD protection devices, and RF ICs; passive components such as resistors, inductors, and capacitors; and functional modules such as display modules, cameras, keypads, speakers, and batteries. PCBs, flexible PCBs (FPCBs), and cases are used in order to interconnect or to embed the components and the modules.

It is impractical to consider everything in the ESD simulations; therefore, proper selections should be made. The selections are made based on the principle that the mobile phone and the HCP form the 3-D capacitor, and the transient ESD current flows through the lowest impedance path. The metallic objects that have a large area and are close to the HCP, such as PCBs, display modules, batteries, and touch panels, become dominant current paths of the ESD current. Objects that act as field coupling paths for the ESD, such as FPCBs and antennas are also selected. The modeling methods for these objects are explained as follows.

1) Modeling of Mobile Phone's Printed Board Assembly: A PCB populated with the active and the passive components and the functional modules is known as a printed board assembly (PBA). By importing the PCB data from PCB design software, the basic ESD simulation model of the PBA is constructed. The lumped elements such as bypassing capacitors, filters, and impedance matching networks are all included in the PBA simulation model.

The coupling level of the ESD current to the signals of the active components is determined by the input impedances of the signals as well as the physical structures of the interconnections. The I/O buffer information specification (IBIS) models provide a way of representing the electrical characteristics of the signals behaviorally [12]. However, it is impractical to use the IBIS models in the ESD simulations because not only the impedance information of the signals but also their *I–V*-time characteristics are embedded in the IBIS models. Only the impedance information of the signals is extracted from the IBIS models and the equivalent circuit models are designed

The equivalent circuit model of the transient voltage suppressor (TVS) diodes has already been published [13]; however, this model is not directly applicable to the ESD simulations because it requires a voltage-controlled voltage source that is not available in the EM software. The voltage-controlled voltage source is used to describe the breakdown voltages of the TVS diodes. In this paper, the TVS diodes are modeled using the lumped resistors under the assumptions that those devices are always in the breakdown operation region and the voltage-to-current characteristics are described by their dynamic resistances. The diode operation regions between the forward turn-on and the reverse breakdown are ignored because the voltage levels of the ESD-sensitive signals are higher than the reverse breakdown voltage of the TVS diode. The parasitic inductance and the junction capacitance of the TVS diodes are all included in the simulation models.

2) Modeling of Mobile Phone's Battery Pack: The battery pack consists of a metallic shield can and internal Li-ion battery cells. Previously published papers on battery pack modeling focus on the battery lifetime analysis [14], which is not applicable to ESD simulations. In this paper, a hybrid battery pack model for the ESD simulations is developed. Because the electrical characteristics of the metallic shield can be influenced by its surroundings, it is modeled using a 3-D object in the ESD simulations. In order to include the electrical characteristics of the battery cells, an equivalent circuit whose parameters are extracted from the measured reflection coefficients (S_{11}) of the battery cells is designed. The 3-D structure and the equivalent circuit are used to describe the electrical characteristics of the shield can and the battery cells, respectively.

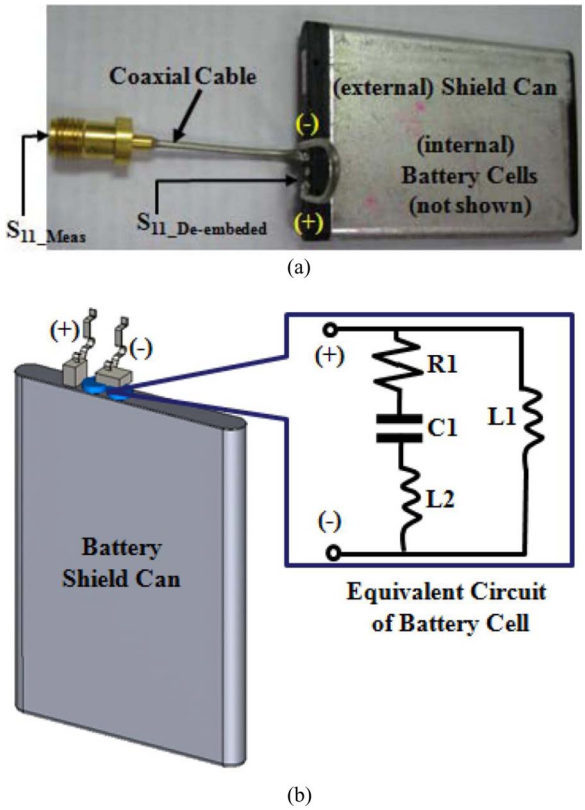

Fig. 6. (a) Battery pack with test fixture. (b) ESD simulation model of battery pack.

Fig. 6(a) shows the battery pack with the coaxial cable, which is used to interface the battery pack with the vector network analyzer; in this figure, S_{11}_Meas and S_{11}_Deembedded represent the measured one-port reflection coefficients at the coaxial cable and the deembedded reflection coefficients at the terminals of the battery pack, respectively. The effects of the coaxial cable are deembedded and the equivalent circuit model is designed using the deembedded reflection coefficients. It is important to note that the shielding can of the battery pack is connected to the plus terminal of the battery pack in order to prevent the corrosion of the shielding can. Fig. 6(b) shows the developed hybrid battery pack model for the ESD simulations, where R1, C1, L1, and L2 are 60 Ω, 18 pF, 11 nH, and 14 nH, respectively.

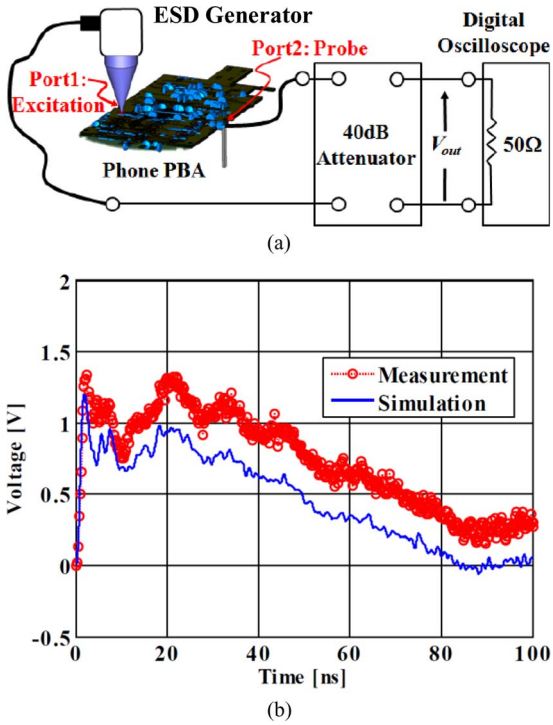

Fig. 7. Experimental verification of simulation models. (a) Schematics of measurement setup. (b) Measured and simulated time-domain waveforms for the GESP case.

3) Experimental Verification of Simulation Models: The accuracy of the developed models for the ESD simulations is experimentally verified. Fig. 7(a) shows the schematics of the measurement setup. In order to minimize the effect of the arc instead of the air discharge mode, the contact mode ESD testing is performed at port 1, and the propagated or the coupled voltage level is monitored at port 2. The 40-dB attenuator is used to protect the digital oscilloscope from the high level of ESD. The charging voltage of the ESD generator is selected as $+1$ kV for experimental verifications. The experimental verifications are carried out for four different combinations: ground excitation and signal probing (GESP), ground excitation and ground probing, signal excitation and signal probing, and signal excitation and ground probing. Fig. 7(b) shows the measured and the simulated time-domain waveforms for the GESP case. The red open circles and the blue solid line represent the measured and the simulated voltage ($V_{\rm out}$), respectively. The measured and the simulated waveforms are quite close to each other, and the difference in peak levels is around 10%. The maximum difference in peak levels for the other cases is less than 20%.

IV. Case Study: Analysis of Mobile Phone's ESD Soft Failure and Design of Countermeasures

The countermeasures against ESD soft failures for a Samsung mobile phone are designed based on the proposed analysis methodology, and the case study is addressed in this section. The mobile phone is of the slide type, one that typically has poor immunity to ESD because there is only a single electrical connection between the sub- and the main-PBAs, which is the FPCB. The ESD current is crowded on the FPCB between the two PBAs, and the signals on the FPCB are easily influenced by the ESD. Fig. 8(a) shows the structure of the slide-type mobile phone.

The detailed analysis steps have already been explained in Section II and are shown in Fig. 2. First, the mobile phone's immunity to the ESD is characterized (STEP-1). The detected ESD soft failure is the freezing of the mobile phone when discharging the ESD generator on the metallic case of the mobile phone, called the "slide lower" in this paper. The ESD generator position is set to the left upper edge of the slide lower, and the injected ESD current waveform is measured (STEP-2) for the ESD simulations.

The next step is to develop the simulation model of the mobile phone (STEP-3). The details of the modeling methods and the method to select the components to be modeled are explained in the previous section. The LCD module, slide lower, battery, sub-PBA, main-PBA, antenna, and FPCB are included in the ESD simulation models, as shown in Fig. 8(a). For brevity, the LCD module is not shown in the figures. The ESD generator is located at the left upper edge of the slide lower, and the active and the passive components are also included in the simulation model.

A commercial time-domain EM field simulator, the CST Microwave Studio from Computer Simulation Technology AG, is used for the ESD simulations (STEP-4). Fig. 8(a) and (b) shows the ESD current distributions on the mobile phone and the backside of the sub-PBA at 1.0 and 1.8 ns, respectively. The yellow and the blue colors represent the highest and the lowest ESD current levels, respectively.

First, the ESD current injected from the ESD generator flows to the slide lower of the mobile phone. Then, the ESD current flows to the sub-PBA via the capacitive coupling path between the sub-PBA and the slide lower. There is one additional current path through the screws at the bottom of the slide lower. As a result, the ESD current is crowded on the sub-PBA, as shown in Fig. 8(b).

The nearest metallic parts to the HCP are the main-PBA and the battery pack, whose terminals are electrically connected to the main-PBA as well. The FPCB that provides the only current path from the sub-PBA to the main-PBA is crowded with the ESD current, as shown in Fig. 8(b). As a result, the signals on the FPCB are easily influenced by the ESD and most of the FPCB areas are marked in yellow.

From the simulation results, the ESD-sensitive signals for which the voltage levels are greatly changed by the ESD current are extracted and are tabulated in Table III. All of the ESD-sensitive signals are on the FPCB. The KEYPAD_ROW(0:1) and the KEYPAD_COL(0/3) are the signals of the baseband modem IC and are used for the keypad operations. The LCD_RESET is used to reset the LCD module and the LCD_DATA(6/14) are the signals of the LCD module for the display data. The RESET_MODEM is used to reset the baseband modem IC and is routed only on the main-PBA. The KEYPAD_COL(0) is also routed only on the main-PBA.

It is important to note that the ESD-sensitive signals are the only probable candidates for the ESD soft failures, i.e., these

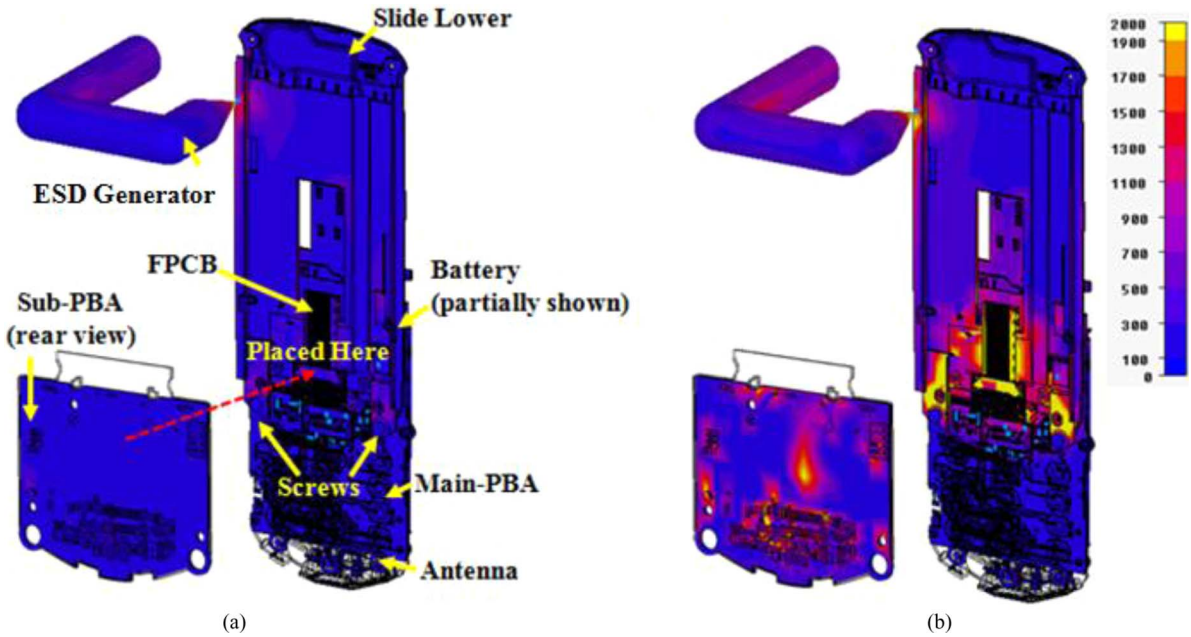

Fig. 8. ESD current distribution on a mobile phone and backside of sub-PBA. (a) 1.0 ns. (b) 1.8 ns.

TABLE III
MONITORED VOLTAGE LEVELS OF IC SIGNALS

	Net	Voltage Level (V) Min	Max	Result of Contact Mode ESD Testing
ESD-sensitive	KEYPAD_ROW(0)	0	85.5	Freezing
	KEYPAD_ROW(1)	0	69.8	Freezing
	KEYPAD_COL(3)	-56.7	41.0	Freezing
	LCD_RESET	-59.5	39.8	No ESD Failure
	LCD_DATA(6)	-58.9	35.9	No ESD Failure
	LCD_DATA(14)	-48.1	31.2	No ESD Failure
Normal (partially listed)	KEYPAD_COL(0)	-7.1	0.9	No ESD Failure
	RESET_MODEM	-1.3	2.2	No ESD Failure

TABLE IV
MONITORED VOLTAGE LEVELS OF IC SIGNALS WITH AND WITHOUT *RC* LOW-PASS FILTERS

	Net	Voltage (V) Without RC Filters (Original) Min	Max	With RC Filters Min	Max
ESD-sensitive	KEYPAD_ROW(0)	0	85.5	0	10.1
	KEYPAD_ROW(1)	0	69.8	0	12.4
	KEYPAD_COL(3)	-56.7	41.0	0	8.9

signals may or may not cause the ESD soft failures. When the logic errors of the ICs occur, the ESD-sensitive signals, actually, cause the ESD soft failures. One-shot simulations of the ESD soft failures would be impossible because a truly comprehensive ESD simulator has not been developed so far; the logic errors of the ICs cannot be predicted using the EM simulators, and the ESD current paths cannot be analyzed using the circuit simulators.

In order to pinpoint which of the ESD-sensitive signals cause ESD soft failures, i.e., the freezing of the mobile phone, ESD testing with the contact discharge mode is performed for the extracted ESD-sensitive signals (STEP-5). The charging voltage of the contact discharge mode is set to be much lower than that of the air discharge mode to prevent physical damages to the ICs. The ESD testing is performed for all of the ESD-sensitive signals; the testing results are tabulated in Table III. Based on the test results, we conclude that the KEYPAD_ROW(0:1) and the KEYPAD_COL(3) signals of the modem IC cause the freezing of the mobile phone while the other ESD-sensitive signals such as the LCD_RESET and the LCD_DATA(6/14) are not associated with ESD soft failures. It is important to note that the ESD simulations are essential because all of the signals should be zapped using the ESD generator if the information on the ESD-sensitive signals from the ESD simulations is not available.

The *RC* low-pass filters are designed for countermeasures against the freezing of the mobile phone, with a series 100-Ω resistor and a shunt 100-pF capacitor and are placed close to the FPCB connector on the main-PBA. 0603-size lumped chip resistors and capacitors are used to implement the *RC* low-pass filters. The largest values of the resistance and the capacitance that meet the signal integrity specifications of the signals are used to design the filters. The simulated voltage levels of the KEYPAD_ROW(0:1) and the KEYPAD_COL(3) signals, both with and without the *RC* low-pass filters, are tabulated in Table IV. As listed in Table IV, the monitored voltage levels are

reduced by more than 82% when the *RC* low-pass filters are implemented. In order to verify that the reduced voltage levels of the pinpointed signals, actually, solve the problem of ESD soft failures, the improved mobile phone's immunity to ESD is characterized again, and no ESD soft failure is detected. In this paper, *RC* low-pass filters are implemented on the mobile phone's PBA; however, implementing *RC* low-pass filters on the modem IC is a fundamental solution to prevent the ESD soft failures.

V. Conclusion

The systematic analysis methodology for the mobile phone's ESD soft failures is proposed in this paper. The proposed analysis methodology consists of two parallel processes: one is the ESD simulation and the other is the ESD characterization of the mobile phone. If a truly comprehensive ESD simulator is available and the ESD current paths and the logic errors of the ICs are, simultaneously, analyzed, then the analysis methodology can be greatly simplified because the characterization steps are not needed. The ESD simulation models that consist of the ESD generator, the ESD testing setup, and the mobile phone are also developed and their accuracy is experimentally verified. The proposed analysis methodology is applied to design the countermeasures against the ESD soft failures of the slide-type mobile phone and the root causes of the ESD soft failures are analyzed. It is found that the signals of the baseband modem IC for the keypad operations cause the freezing of the mobile phone. The *RC* low-pass filters are designed with the series 100-Ω resistors and the shunt 100-pF capacitors and are implemented on the main-PBA of the mobile phone. The ESD simulation results of the improved mobile phone show more than 82% voltage-level reductions of the signals, which cause the ESD soft failure. In order to verify that the reduced voltage levels of the pinpointed signals actually solve the problem of ESD soft failures, the improved mobile phone's immunity to ESD is characterized again, and no ESD soft failure is detected.

References

[1] R. R. Tummala, "SoP: What is it and why? A new microsystem-integration technology paradigm—Moore's law for system integration of miniaturized convergent systems of the next decade," *IEEE Trans. Adv. Packag.*, vol. 27, no. 2, pp. 241–249, May 2004.

[2] *Recommended ESD Target Levels for HBM/MM Qualification,* JEDEC Publication JEP155, Aug. 2008.

[3] M. Ramdani, E. Sicard, A. Boyer, S. Ben Dhia, J. J. Whalen, T. H. Hubing, M. Coenen, and O. Wada, "The electromagnetic compatibility of integrated circuits—Past, present, and future," *IEEE Trans. Electromagn. Compat.*, vol. 51, no. 1, pp. 78–100, Feb. 2009.

[4] J. E. Vinson, J. C. Bernier, G. D. Croft, and J. J. Liou, *ESD Design and Analysis Handbook*. Boston, MA: Kluwer, 2003, p. 48.

[5] G. Muchaidze, J. Koo, Q. Cai, T. Li, L. Han, A. Martwick, K. Wang, J. Min, J. L. Drewniak, and D. Pommerenke, "Susceptibility scanning as a failure analysis tool for system-level electrostatic discharge (ESD) problems," *IEEE Trans. Electromagn. Compat.*, vol. 50, no. 2, pp. 268–279, May 2008.

[6] *EMC—Part 4-2: Testing and Measurement Techniques—Electrostatic Discharge Immunity Test,* IEC 61000-4-2 International Standard, International Electrotechnical Commission (IEC), Geneva, Switzerland, 2001.

[7] (2010). [Online]. Available: http://www.noiseken.com/modules/products/index.php/content0181.html

[8] F. Centola, D. Pommerenke, K. Wang, T. V. Doren, and S. Caniggia, "ESD Excitation Model for Susceptibility Study," in *Proc. IEEE Int. Symp. Electromagn. Compat.*, Aug. 18–22,, 2003, pp. 58–63.

[9] (2010). [Online]. Available: http://www2.tek.com/cmswpt/psdetails.lotr?ct=PS&cs=psu&ci=13406&lc=EN

[10] (2008). [Online]. Available: http://www.minicircuits.com/cgi-bin/modelsearch?model=BW-40N100W

[11] (2004). [Online]. Available: http://www.fischercc.com/Quadrary-Pages/Current-Probes/F-65.htm

[12] (2005). [Online]. Available: http://www.vhdl.org/pub/ibis/cookbook/cookbook-v4.pdf

[13] J. Lepkowski and W. Lepkowski, "Evaluating TVS protection circuits with SPICE," *Power Electron. Technol.*, vol. 5, no. 1, pp. 44–49, Jan. 2006.

[14] M. Chen and G. A. Rincón-Mora, "An accurate electrical battery model capable of predicting runtime and *I–V* performance," *IEEE Trans. Energy Convers.*, vol. 21, no. 2, pp. 504–511, Jun. 2006.

Ki Hyuk Kim (M'05) received the Ph.D. degree in electronics engineering from Korea University, Seoul, Korea, in 2005.

From 2001 to 2005, he was at Solid Technologies, Inc., Seoul, where he was involved in the research and development of mobile communication equipments for (W) code division multiple access and Wibro, as a R&D Staff Member. He was a Postdoctoral Researcher in the Department of Electrical and Computer Engineering, University of Illinois, Urbana-Champaign, from 2005 to 2007. He is currently at Advanced CAE Laboratory, Digital Media and Communications R&D Center, Samsung Electronics Company, Ltd., Suwon, Korea. His research interests include design of mixed-signal ICs, signal-/power-integrity of high-speed systems, and improvements of system-level electrostatic discharge problems.

Yongsup Kim, photograph and biography not available at the time of publication.